Research Article

Experimental investigation of nozzle angle effects on the brine discharge by inclined dense jets in stagnant water ambient

Mohammad Azizi[1] · Davood Goharikamel[1] · Fereidon Vafaei[1]

Received: 4 March 2020 / Accepted: 1 August 2020 / Published online: 10 August 2020
© Springer Nature Switzerland AG 2020

Abstract
This study presents a series of laboratory experiments conducted on inclined dense jets from 15° to 90° at 15° intervals, which discharge brine in a stagnant water ambient. The main geometrical properties and dilution of the flow were measured by light attenuation method. The densimetric Froude number is an effective dimensionless parameter on the inclined dense jet behavior that changes with initial velocity and the brine density. In this study, attempts have been made to investigate the relationship between the main geometric parameters of flow and dilution at return point, so a parameter is defined as the dimensionless trajectory length (R_L). The results show that dilution at the return point is somewhat related to the dimensionless trajectory length, specifically for a specific Froude number, the highest dilution occurs at about 60° toward the horizontal, while the maximum dimensionless trajectory length occurs between 60° and 75°. Brine deposition on the seabed can create a stable stratification, which can be hazardous to the marine environment, so it is important to maximize dilution. The results of this study are presented as dimensionless diagrams that can be useful to design, estimate, and optimize the outfall systems on large scales.

Keywords Sewage · Desalination · Inclined jet · Dense · Brine discharge · Dilution

List of symbols

D_0	Nozzle diameter
U_0	Initial jet velocity
Q	Discharge rate
Z_{max}	Maximum height of rise
X_C	Distance of centerline return point
g	Acceleration of gravity
g'	Modified acceleration of gravity
F_0	Densimetric Froude number
S	Dilution in a particular point
S_i	Dilution in the centerline return point
C_0	Salinity of the initial brine
C_a	Salinity of the ambient
C	Salinity of the particular point
R_X	Constant factor for return point
R_Z	Constant factor for maximum height
G_θ	Ratio of measuring centerline length
R_L	Dimensionless parameter of trajectory length
K	Constant factor for dilution
θ_0	Discharge angle (toward the horizontal)
ρ_0	Initial brine density
ρ_a	Ambient density

1 Introduction

Nowadays, the scarcity of freshwater for drinking, agriculture, and some industries has become a global concern. As the population grows, this crisis will rise further in the future; therefore, using desalination plants is an effective solution that can produce freshwater from seawater [6]. In all kinds of desalination processes, eventually, a large quantity of brine sewage is discharged into the marine environment by different types of outfall systems. This

✉ Mohammad Azizi, mohammadazizi@email.kntu.ac.ir | [1]Present Address: Department of Civil and Environmental Engineering, Civil Engineering Faculty, K. N. Toosi University of Technology, No. 1346, Vali Asr Street, Mirdamad Intersection, Tehran 1996715433, Iran.

brine sewage contains a high amount of salts and several chemical materials that make the sewage heavier than seawater; so this sewage tends to settle on the seabed and form a stable stratification of brine and other contaminants. This phenomenon may cause harmful impacts on the marine ecosystem [10, 16]. The use of inclined jets is one of the discharge methods that can reduce these hazards by mixing and dilution processes. Because the brine sewage is heavier than seawater, it is preferable to discharge the sewage upward, to increase the trajectory and consequently achieve better dilution at the return point [3].

In recent decades, extensive researches have been conducted on both the geometry and the dilution parameters of inclined dense jets, which investigated the behavior of jets in different conditions of nozzle and ambient. Numerous researches have been done about optimum nozzle orientation in the single port inclined dense jets [8, 14, 15, 17–22, 24, 25, 27]. A notable disagreement is visible for the dilution at the return point in the previous studies, but these studies generally showed that the highest dilution at the return point occurs at about 60°. Studies on the effects of the bottom slope showed that, by increasing the slope from 0° to 30°, the optimum angle decrease from 60° to about 40° [12]. Also, some studies have been carried out on the patterns of concentration and velocity distribution in cross sections of the dense effluent trajectories; the results show that the distribution is essentially Gaussian for jets when the momentum flux is dominant. However, it is reported to be half Gaussian for surface discharges or Semi Gaussian for inclined dense jet flows when the buoyancy flux is dominant, actually, the concentration distribution deviates from the Gaussian in the lower part because dense fluid detaches from the jet flow [1, 9, 11, 21, 23, 28]. Several studies have been conducted on multiport outfall systems to determine the optimal distance and arrangement of nozzles [2, 26, 30]. The buoyancy behavior of thermal-saline effluent has also been investigated [4]. Besides the experimental studies, mathematical and numerical modeling have been considered [5, 13, 18, 19, 31] and commercial software such as CORMIX, CORJET and VISJET have been developed, but the experimental results are still the basis of estimating the prototype behavior.

The simplest experimental model for inclined dense jet is a single port jet that discharges the brine (ρ_0) through a D_0 diameter nozzle with U_0 velocity into a stagnant ambient ($\rho_a < \rho_0$) at θ_0 angle toward the horizontal (Fig. 1).

In inclined dense jets, when the jet enters the water ambient, the momentum flux is dominant and the jet moves upward; then, by reduction of the flow velocity, the vertical momentum flux fades out and the buoyancy flux dominates [29]. Therefore, the jet turns into a plume and after reaching to the maximum height, it starts to move downward until hitting the bottom. In the flow trajectory, the line with the highest concentration is called centerline and is obtained from time-averaged image. In each of the cross sections of the flow, the point that has maximum concentration (bolder color) is one point of the centerline. The set of these points forms the centerline of the trajectory. The length of the centerline (L_C) is used as the length of the flow path.

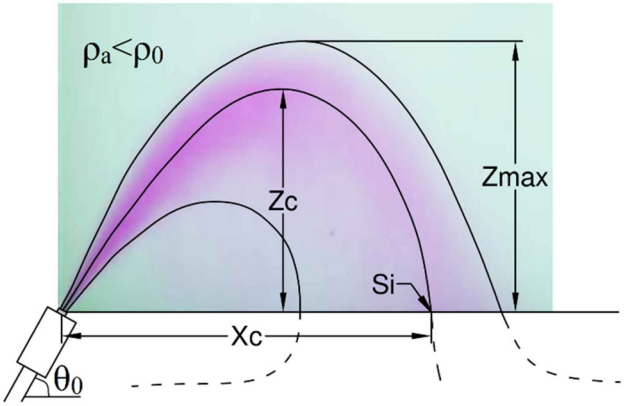

Fig. 1 Schematic and time-averaged image of an inclined dense jet modeled in the laboratory for this study

The maximum height of rise (Z_{max}) and the distance of centerline return point to the nozzle level (X_C) are important geometrical parameters of the flow trajectory [7]. The flow behavior is controlled by a dimensionless number that is defined as the initial densimetric Froude number (F_0):

$$F_0 = \frac{u_0}{\sqrt{g'.D_0}} \tag{1}$$

$$g' = \frac{g(\rho_0 - \rho_a)}{\rho_0} \tag{2}$$

The g' is the modified acceleration of gravity. For densimetric Froude numbers greater than about 20, the normalized trajectory of the flow is a function of the nozzle angle [15]; therefore, this principle also includes the maximum height of upper boundary (Z_{max}) and the distance of return point (X_C), and these can be presented in the following forms:

$$R_Z = \frac{Z_{max}}{D_0.F_0} \tag{3}$$

$$R_X = \frac{X_C}{D_0.F_0} \tag{4}$$

In this study, an attempt has been made to extract a parameter (G_θ) that can be used to estimate the trajectory length with having the X_C and the Z_{max}. This parameter is defined as follows:

$$G_\theta = \frac{L_C}{(X_C + Z_{max})} \tag{5}$$

where L_C is the length of the centerline that obtained from each experiment.

The dilution (S) at a particular point of the flow is defined as the ratio of the initial salinity of the brine (C_0) to the salinity(C) of that point of the flow:

$$S = \frac{(C_0 - C_a)}{(C - C_a)} \tag{6}$$

where C_a is the salinity of the ambient.

The dilution can be normalized by F_0 and becomes a function of the nozzle angle (θ_0) [29]. The minimum dilution at the return point (S_i) occurs in the centerline and can be presented in the following form:

$$k = \frac{S_i}{F_0} \tag{7}$$

Considering the fact that many animals and plants live on the seabed, the angle that causes the greatest dilution at the return point is the optimum angle to minimize the environmental hazards of brine disposal in the marine environment. In the following, the effects of nozzle orientation on dilution and geometrical parameters of the inclined dense jets are investigated for a comprehensive series of nozzle angles by light attenuation method. The results are compared with other available studies. Furthermore a parameter is defined as dimensionless length of the trajectory (R_L) and its relationship with the geometry and dilution of the flow has been investigated.

2 Methodology

2.1 Experimental setup

In the current study, an experimental model has been made with the following description. A glass tank, 2 m long, 2 m wide and 1.2 m high, was used for simulating the sea ambient in the experiments (Fig. 2). To prepare the brine, a smaller tank with a capacity of 0.3 m^3 is placed approximately 3 m above the ambient tank. There is a mixer in the brine tank to mix salt (NaCl) and water. Also, to observe the effluent path, a color detector (Rhodamine) is mixed with the brine in this tank. An overflow container is located near the brine tank to provide the constant head.

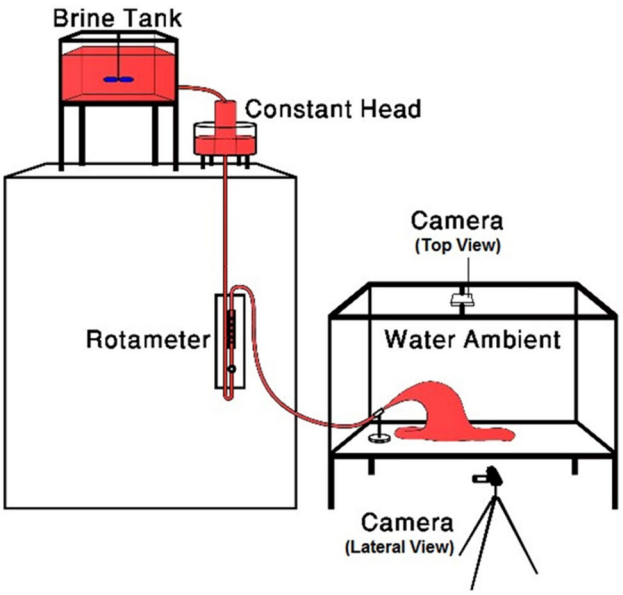

Fig. 2 Schematic of experimental setup

There is a rotameter between the constant head and the nozzle to adjust the discharge rate by a regulation valve, therefore the initial densimetric Froude number is adjustable by changing two parameters: the discharge velocity and the brine salinity. The diameter of the nozzle is 4 mm and the discharge angle is adjustable; the nozzle is located 30 cm above the bottom of the ambient so that the boundary conditions don't affect the flow behavior. To measure the salinity of the brine and water ambient before each experiment, a portable multimeter (Hach) with a precision of 0.1 psu is used. The brine and water densities are measured by hydrometers with an accuracy of 0.1 kg/m^3. To record the flow path, a full HD camera with the ability to recording 30 frame per second video is used, which is located at a distance of 3 m from the ambient; the manual setting is used on this camera to keep the focus from changing during the experiment. Another camera is used to record the experiment from above in order to measure the lateral spreading of the flow at the return point. The experiments are performed in a dark room and a luminous sheet is used in the backside of the ambient to increase the recording quality.

2.2 Calibration

In each experiment, a time-average image is provided from 45 s of the brine discharging by MATLAB image processing (Fig. 3). The geometrical parameters are extracted from the processed images. In particular, to find the centerline, a MATLAB image processing code was used, in which a desired number of cross sections perpendicular to

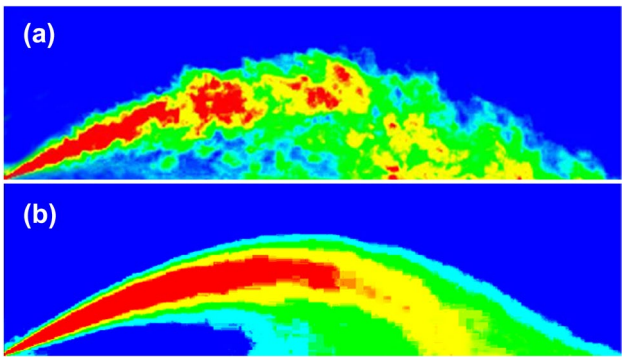

Fig. 3 MATLAB image processing (30° jet): **a** instantaneous image. **b** Time-averaged image

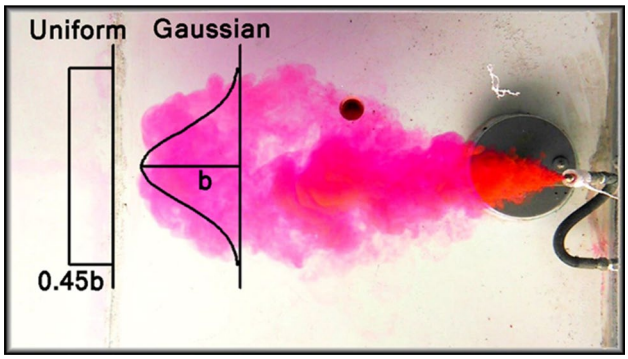

Fig. 4 Top view to measure lateral spreading at return point

the flow path was manually generated. The darkest points in each cross section were defined as points of the centerline, in the form of a broken line. This was converted to a smooth centerline by fitting a SP line in AutoCAD software and its length was obtained by using "list" command.

In this research, the light attenuation method is used to obtain the dilutions. So the dilutions at the return point are obtained from calibration of the light intensity in gray time-averaged images with the salinity. To achieve this purpose, at first the 2D light intensity (uniform cross-sectional profile) obtained from lateral camera should convert to the 3D (Gaussian cross-sectional profile). In order to achieve this purpose it is necessary to know the lateral spreading of the plume in the return point. Therefore, to determine the lateral spreading of the plume at the return point, the flow of the brine is recorded by a camera from above. Due to the simultaneous videos recording in both of the top and the side views, the lateral spreading of the plume can be obtained at the moment of the arrival to the return point. In other words, when in the lateral camera point of view the brine reaches the return point, the lateral spreading of the plume is measurable from the top camera point of view. According to the symmetry of the concentration in cross section of the flow, the distribution of the concentration is Gaussian. Due to the fact that lateral imaging has been done in 2D form, instead of the Gaussian profile, a uniform profile (with the same thickness and area) is used, because the light intensity is the same for both profiles. Thus, if the concentration peak point in the Gaussian profile is *b*, the concentration in the uniform profile is approximately 0.45*b*. This method is only for finding the concentration at the return point and is assumed that the lateral spreading of the plume is equal to the width of the Gaussian profile (Fig. 4).

According to the facilities in this study, measuring of the salinity at the return point was not possible, but by using a method that will be explained, the salinity is obtained by the light intensity at the return point. For calibration of the light intensity and the brine salinity, two glass cubical containers with widths of 20 and 40 cm (in the range of lateral spreading of plumes at the return point) are used. Because the lateral spreading of the plumes at the return point are different in the experiments, thus two glass containers with different thicknesses have been used so that the effect of the lateral spreading of the plume on the light intensity can be measurable by interpolation. To find the equivalent salinity of any light intensity, after each experiment, the glass cubical containers are filled with the brine. By adding clear freshwater in the containers, the reduction of the salinity and the light intensity is recorded, by Hach multimeter and video camera, respectively. All images are turned into gray in image processing. In the gray images, a number between 0 and 255 is assigned to each pixel, 0 assigned to absolute black and

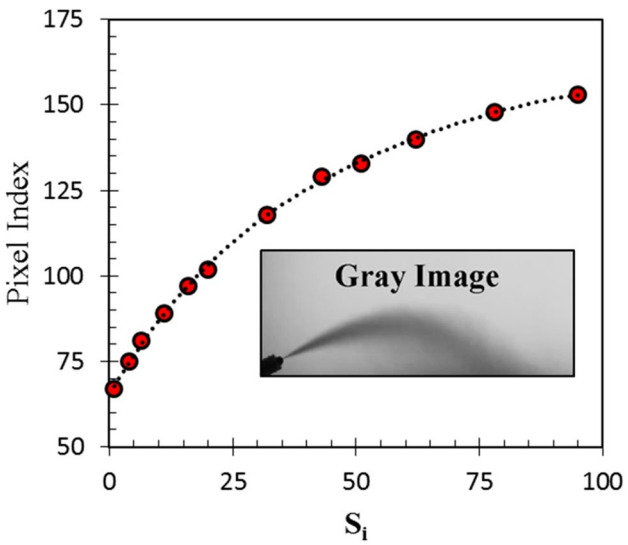

Fig. 5 Calibration curve of dilution and light intensity

255 assigned to absolute white. Eventually, the salinity of uniform profiles is obtained considering the interpolation of the plume thickness. These values are 0.45 of the Gaussian distribution peak point (salinity of centerline in the return point). Then, the dilutions are achieved by considering the salinities of the initial brine, the ambient and the return point (according Eq. 6). An example of typical curve obtained from light intensity (pixel index in gray image) and dilution is shown in Fig. 5.

Table 1 The main experimental specifications and parameters

No	θ_0 (°)	$\rho_0-\rho_a$ (kg/m^3)	ρ_0 (kg/m^3)	Q (m^3/s)	F_0	X_C (m)	Z_{max} (m)	L_C (m)	G_θ	S_i
1	15	118.2	1117.7	0.0000274	19.3	0.173	0.046	0.187	0.853	10
2	15	56.5	1056.0	0.0000391	32.7	0.254	0.078	0.282	0.849	19
3	15	83.8	1083.3	0.0000500	38.1	0.318	0.088	0.348	0.856	30
4	15	118.2	1117.7	0.0000649	45.7	0.328	0.095	0.362	0.856	41
5	15	56.5	1056.0	0.0000608	50.8	0.402	0.102	0.431	0.855	37
6	15	83.8	1083.3	0.0000740	56.4	0.426	0.125	0.470	0.853	48
7	30	115.2	1114.7	0.0000267	18.9	0.245	0.065	0.264	0.852	15
8	30	57.3	1056.8	0.0000330	27.5	0.378	0.102	0.406	0.846	35
9	30	90.3	1089.8	0.0000455	34.1	0.420	0.137	0.470	0.844	33
10	30	115.2	1114.7	0.0000579	41.0	0.455	0.144	0.513	0.856	35
11	30	57.3	1056.8	0.0000574	47.8	0.501	0.193	0.591	0.852	48
12	30	90.3	1089.8	0.0000725	54.3	0.605	0.204	0.697	0.862	44
13	30	122.8	1122.3	0.0000853	59.6	0.687	0.210	0.771	0.860	65
14	45	123.2	1122.7	0.0000321	22.4	0.282	0.134	0.364	0.875	25
15	45	61.4	1060.9	0.0000349	28.6	0.333	0.185	0.451	0.871	37
16	45	83.7	1083.2	0.0000469	35.7	0.473	0.200	0.583	0.866	35
17	45	100.6	1100.1	0.0000568	41.5	0.496	0.219	0.620	0.867	55
18	45	123.2	1122.7	0.0000673	47.0	0.583	0.274	0.754	0.880	74
19	45	61.4	1060.9	0.0000670	54.9	0.625	0.309	0.828	0.887	82
20	45	100.6	1100.1	0.0000786	57.4	0.694	0.353	0.918	0.877	76
21	45	83.7	1083.2	0.0000850	64.8	0.742	0.383	0.993	0.883	95
22	60	122.7	1122.2	0.0000289	20.2	0.224	0.160	0.355	0.924	26
23	60	109.4	1108.9	0.0000372	26.7	0.245	0.203	0.419	0.935	31
24	60	55.6	1055.1	0.0000395	33.1	0.329	0.326	0.609	0.930	44
25	60	81.9	1081.4	0.0000515	39.4	0.418	0.343	0.705	0.926	48
26	60	122.7	1122.2	0.0000648	45.3	0.449	0.409	0.788	0.918	71
27	60	109.4	1108.9	0.0000727	52.1	0.546	0.424	0.896	0.924	84
28	60	55.6	1055.1	0.0000679	56.9	0.565	0.510	0.994	0.925	76
29	60	81.9	1081.4	0.0000816	62.5	0.636	0.523	1.074	0.927	90
30	75	106.2	1105.7	0.0000287	20.7	0.119	0.211	0.366	1.109	19
31	75	57.1	1056.6	0.0000304	25.3	0.173	0.225	0.437	1.098	35
32	75	84.1	1083.6	0.0000457	34.8	0.210	0.328	0.585	1.087	46
33	75	125.7	1125.2	0.0000563	39.1	0.263	0.394	0.723	1.100	40
34	75	106.2	1105.7	0.0000646	46.6	0.290	0.418	0.770	1.088	70
35	75	57.1	1056.6	0.0000612	51.0	0.336	0.473	0.895	1.106	64
36	75	84.1	1083.6	0.0000738	56.2	0.365	0.553	1.013	1.103	69
37	90	108.2	1107.7	0.0000301	21.6	0.000	0.170	–	–	–
38	90	61.9	1061.4	0.0000349	28.5	0.000	0.231	–	–	–
39	90	86.4	1085.9	0.0000446	33.7	0.000	0.258	–	–	–
40	90	108.2	1107.7	0.0000552	39.7	0.000	0.328	–	–	–
41	90	61.9	1061.4	0.0000554	45.3	0.000	0.397	–	–	–
42	90	86.4	1085.9	0.0000693	52.4	0.000	0.447	–	–	–

3 Results and analysis

3.1 Experimental data

In the present study attempts have been made to ensure that the initial parameters and nozzle angles have sufficient diversity and include appropriate range of densimetric Froude numbers. For each nozzle angle, at least 6 experiments have been carried out in various salinities. The specifications of each experiment and the extracted parameters are presented in Table 1. The experiments have been carried out in the range of densimetric Froude number from about 19 to about 62 and the angle of nozzle was set between 15° and 90° by 15° intervals.

3.2 Geometrical parameters

The relation of the normalized return point distance (X_C/D_0) and the densimetric Froude number is presented in Fig. 6. For each nozzle orientation, the normalized return point distance has a significant linear relation with the dens metric Froude number ($X_C/D_0 = R_X.F_0$). Comparisons of the results of this study with the results of other researches are presented quantitatively in Table 2; furthermore, Fig. 7 indicates the R_X values for the various nozzle orientations. Two points, 0° and 90°, have zero distance for obvious physical reasons.

The relation of the normalized maximum height of rise (Z_{max}/D_0) and the densimetric Froude number is illustrated in Fig. 8. This indicates a simple linear function between normalized maximum height and dens metric Froude number ($Z_{max}/D_0 = R_Z.F_0$). The results of R_Z values that obtained in this research and in other studies are presented in Table 3 and Fig. 9.

The G_θ coefficient is in range of 0.84–1.11 that are presented in Table 1 for each experiment, According to the self-similarity of the trajectory at each angle, the average of these values is given in Table 4. According to Eq. 5, the parameter of G_θ can relate the length of the centerline (L_C) to X_C and Z_{max}.

3.3 Dilution at the return point

The following diagram (Fig. 10) indicates that there is an approximately linear function between return point dilution and densimetric Froude number ($S_i = K.F_0$) with an acceptable correlation coefficient. The values of K are presented in Table 5 for 15°, 30°, 45°, 60° and 75° angles. The dilution in return point is not measurable for 90°. In Fig. 11, the K values of this study are compared with the results of other researches. These results are sufficiently in line with other studies, although, there are slight differences which could be due to the variety of research methods and other initial conditions, such as salinity, temperature, turbulence, nozzle diameter and distance of nozzle from the bottom (boundary effects).

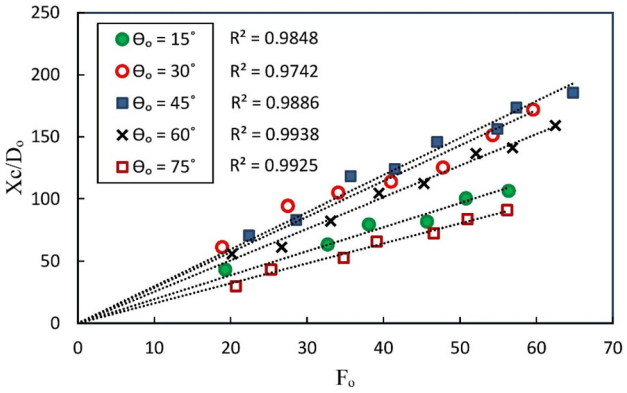

Fig. 6 Relation of normalized return point distance with densimetric Froude number at different angles

Table 2 Results of R_X in this study and other researches

Study	15°	30°	45°	60°	75°
This study	1.94	2.86	2.97	2.53	1.61
Abessi and Roberts [3]	2.97	3.56	3.56	3.04	1.94
Cipollina et al. [8]	–	3.03	2.82	2.25	–
Kikkert et al. [14]	2.13	3.07	3.2	2.8	–
Shao and Law [28]	–	3.00	3.33	–	–
Papakonstantis et al. [21]	–	–	3.16	2.75	1.80
Lai and Lee [15]	2.41	3.18	3.34	2.84	–

4 Discussion

In Fig. 9, a decline is visible in the maximum height at about 75° due to the fallout effect and the interaction of the velocity vectors; this result is adequately in accordance with other studies. Figures 7 and 9 show that the maximum return point distance (X_C) occurred at about 45° and the maximum height of rise (Z_{max}) happened at about 75°, but in discharge of brine sewage, the length of the trajectory is important. Therefore, the relationship between trajectory length and dilution rate has been investigated.

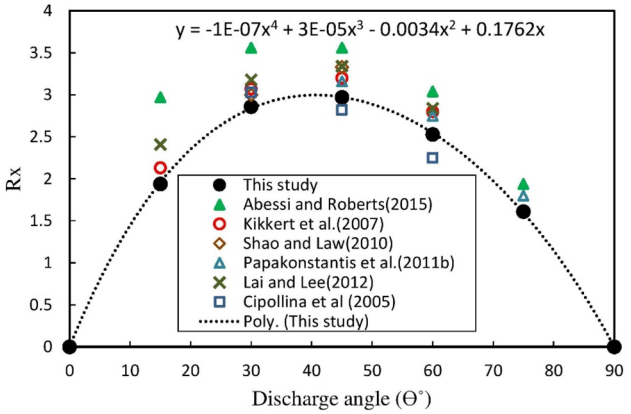

Fig. 7 R_X for various nozzle angles and comparison with previous studies

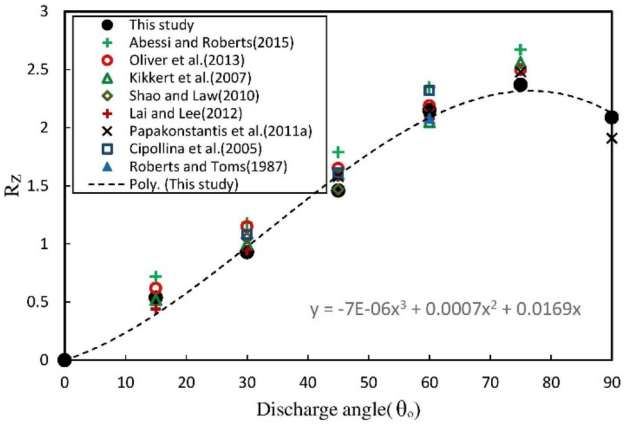

Fig. 9 R_Z for various nozzle angles and comparison with previous studies

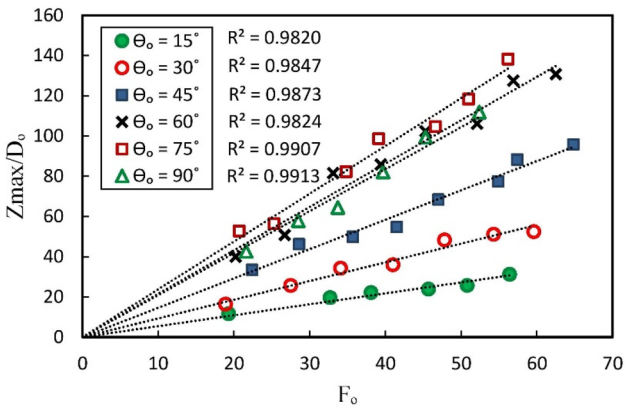

Fig. 8 Relation of normalized maximum height with densimetric Froude number at different angles

In this research a dimensionless parameter of trajectory length (R_L) is defined as an appropriate parameter to estimate the length of the flow. So it is possible to obtain a relatively accurate value of the length of trajectory by using the following equation:

$$R_L = G_\theta\left(R_X + R_Z\right) = \frac{L_c}{Z_{max} + X_c} \cdot \frac{Z_{max} + X_c}{D_0 F_0} = \frac{L_c}{D_0 F_0} \quad (8)$$

It is worth mentioning that it is not possible to determine the exact length of the centerline (L_C) at angle of 90° because despite the maximum height of rise (Z_{max}) is recognizable, the highest point of the centerline (Z_C) is not recognizable in this angle, but considering that at angle of 90°, the fallout effect is maximum and also the X_C is zero, surely the length of trajectory at this angle is less than the length of trajectory at 75°.

As can be seen in Fig. 12, the maximum length of the trajectory occurs between 60° and 75°; but the maximum dilution occurs at about 60°. These results show that the maximum length of the trajectory has a minor difference with the maximum dilution that is due to the decrease of diffusion at higher angles. It can be concluded that although the maximum length of the path is created at an angle between 60° and 75°, but the nozzle angle at about 60° has a better performance in dilution of the brine.

Table 3 Results of R_Z in this study and other researches

Study	15°	30°	45°	60°	75°	90°
This study	0.54	0.93	1.46	2.15	2.37	2.09
Abessi and Roberts [3]	0.72	1.18	1.79	2.35	2.67	–
Roberts and Toms [24]	–	–	–	2.08	–	–
Cipollina et al. [8]	–	1.08	1.61	2.32	–	–
Kikkert et al. [14]	0.52	1	1.6	2.05	2.56	–
Shao and Law [28]	–	1.05	1.47	–	–	–
Papakonstantis et al. [20]	–	–	1.58	2.14	2.48	1.91
Lai and Lee [15]	0.44	0.95	1.58	2.08	–	–
Oliver et al. [18, 19]	0.62	1.15	1.65	2.19	2.5	–

Table 4 The average of G_θ at each angle

Angle (θ)	15°	30°	45°	60°	75°
G_θ	0.854	0.854	0.877	0.926	1.099

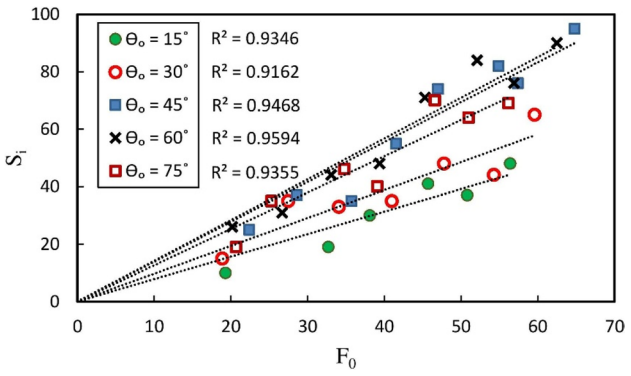

Fig. 10 Relation of dilution with densimetric Froude number at different angles

Table 5 Results of normalized return point dilution (S_i/F_0) in this study and other researches

Study	15°	30°	45°	60°	75°
This study	0.84	0.97	1.39	1.42	1.26
Abessi and Roberts [3]	0.74	1.23	1.65	1.79	1.50
Nemlioglu and Roberts [17]	1.40	1.90	1.70	1.70	1.80
Shao and Law [28]	–	1.45	1.26	–	–
Papakonstantis et al. [21]	–	–	1.55	1.68	1.67
Lai and Lee [15]	0.43	0.82	1.09	1.07	–
Oliver et al. [18, 19]	0.49	0.84	1.22	1.56	1.54

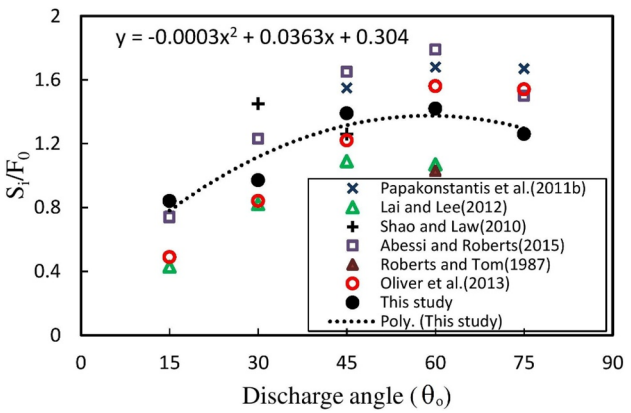

Fig. 11 Return point dilution for various nozzle angles and comparison with previous studies

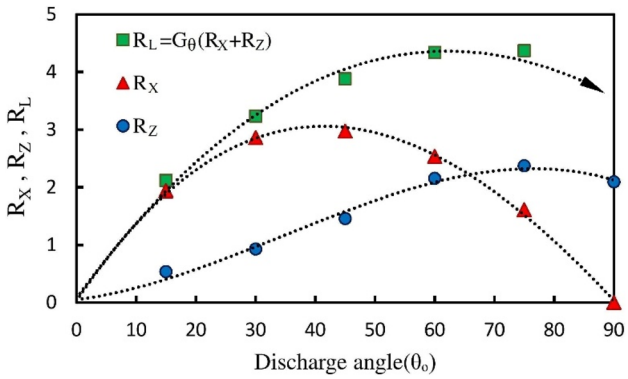

Fig. 12 Parameter of trajectory length ($R_L = G_\theta (R_X + R_Z)$)

5 Conclusion

Several experiments are performed to investigate the nozzle orientation effects on the geometry and dilution behavior of the inclined dense jets, to find the optimum angle that causes the least hazard to marine environment. The results show that the maximum distance of the centerline return point (X_C) occurs at about 45˚, the maximum height of rise occurs at about 75˚ and a decline in the height of rise is observed for higher angles (fallout effect). To find the relationship between trajectory length and dilution rate, a parameter is defined as R_L to express the dimensionless length of the trajectory. The maximum value of R_L occurs between 60° and 75°, but according to the experimental results for maximum dilution that occurs at 60°, it can be said that discharging the brine sewage at about 60˚ and by greater Froude number can cause more dilution, so is preferable for outfall systems.

Acknowledgements This research was carried out at the Water Research Institute of Iran. The authors of this paper would like to thank the staff of the institute, especially Dr. Hossein Ardalan for his boundless assistance.

Compliance with ethical standards

Conflict of interest This research is related to the *Master's* thesis of the corresponding author and there is no conflict.

References

1. Abessi O, Saeedi M, Bleninger T, Davidson M (2012) Surface discharge of negatively buoyant effluent in unstratified stagnant water. J Hydro-Environ Res 6(3):181–193. https://doi.org/10.1016/j.jher.2012.05.004
2. Abessi O, Roberts PJW (2017) Multiport diffusers for dense discharge in flowing ambient water. J Hydraul Eng. https://doi.org/10.1061/(ASCE)HY.1943-7900.0001279

3. Abessi O, Roberts PJW (2015) Effect of nozzle orientation on dense jets in stagnant environments. J Hydraul Eng 141(8):1–8. https://doi.org/10.1061/(ASCE)HY.1943-7900.0001032
4. Ardalan H, Vafaei F (2018) Hydrodynamic classification of submerged thermal-saline inclined single-port discharges. Mar Pollut Bull 130(March):299–306. https://doi.org/10.1016/j.marpolbul.2018.03.052
5. Ardalan H, Vafaei F (2019) CFD and experimental study of 45° inclined thermal-saline reversible buoyant jets in stationary ambient. Environ Process 6(1):219–239. https://doi.org/10.1007/s40710-019-00356-z
6. Belkin N, Kress N, Berman-Frank I (2018) Microbial communities in the process and effluents of seawater desalination plants. In: Sustainable desalination handbook: plant selection design and implementation. Elsevier, Amsterdam, pp 465–488. https://doi.org/10.1016/B978-0-12-809240-8.00012-5
7. Christodoulou GC, Papakonstantis IG, Nikiforakis IK (2015) Desalination brine disposal by means of negatively buoyant jets. Desalin Water Treat 53(12):3208–3213. https://doi.org/10.1080/19443994.2014.933039
8. Cipollina A, Brucato A, Grisafi F, Nicosia S (2005) Bench-scale investigation of inclined dense jets. J Hydraul Eng 131(11):1017–1022. https://doi.org/10.1061/(ASCE)0733-9429(2005)131:11(1017)
9. Crowe A.T, Davidson MJ, Nokes RI (2012) Maximum height and return point velocities of desalination brine discharges. In: Proceedings of the 18th Australasian fluid mechanics conference, AFMC 18–21 December 2012
10. Iso S, Suizu S, Maejima A (1994) The lethal effect of hypertonic solutions and avoidance of marine organisms in relation to discharged brine from a destination plant. Desalination 97(1):389–399. https://doi.org/10.1016/0011-9164(94)00102-2
11. Jiang M, Law AWK, Zhang S (2018) Mixing behavior of 45° inclined dense jets in currents. J Hydro-Environ Res 18:37–48. https://doi.org/10.1016/j.jher.2017.10.008
12. Jirka GH (2008) Improved discharge configurations for brine effluents from desalination plants. J Hydraul Eng 134(1):116–120. https://doi.org/10.1061/(ASCE)0733-9429(2008)134:1(116)
13. Kheirkhah HG, Mohammadian A, Nistor I, Qiblawey H (2015) Numerical modeling of 30° and 45° inclined dense turbulent jets in stationary ambient. Environ Fluid Mech 15(3):537–562. https://doi.org/10.1007/s10652-014-9372-1
14. Kikkert GA, Davidson MJ, Nokes RI (2007) Inclined negatively buoyant discharges. J Hydraul Eng 133(5):545–554. https://doi.org/10.1061/(ASCE)0733-9429(2007)133:5(545)
15. Lai CCK, Lee JHW (2012) Mixing of inclined dense jets in stationary ambient. J Hydro-Environ Res 6(1):9–28. https://doi.org/10.1016/j.jher.2011.08.003
16. Lattemann S, Höpner T (2008) Environmental impact and impact assessment of seawater desalination. Desalination 220(1–3):1–15. https://doi.org/10.1016/j.desal.2007.03.009
17. Nemlioglu S, Roberts PJW (2006) Experiments on dense jets using 3D Laser-Induced Fluorescence (3DLIF).In: Proceedings of the 4th international conference on marine waste water disposal and marine environment, Antalya
18. Oliver CJ, Davidson MJ, Nokes RI (2013) Behavior of dense discharges beyond the return point. J Hydraul Eng 139(12):1304–1308. https://doi.org/10.1061/(ASCE)HY.1943-7900.0000781
19. Oliver CJ, Davidson MJ, Nokes RI (2013) Removing the boundary influence on negatively buoyant jets. Environ Fluid Mech 13:625–648. https://doi.org/10.1007/s10652-013-9278-3
20. Papakonstantis IG, Christodoulou GC, Papanicolaou PN (2011) Inclined negatively buoyant jets 1: geometrical characteristics. J Hydraul Res 49(1):3–12. https://doi.org/10.1080/00221686.2010.537153
21. Papakonstantis IG, Christodoulou GC, Papanicolaou PN (2011) Inclined negatively buoyant jets 2: concentration measurements. J Hydraul Res 49(1):13–22. https://doi.org/10.1080/00221686.2010.542617
22. Papakonstantis IG, Tsatsara EI (2018) Trajectory characteristics of inclined turbulent dense jets. Environ Process 5:539–554. https://doi.org/10.1007/s40710-018-0307-6
23. Papakonstantis IG, Tsatsara EI (2019) Mixing characteristics of inclined turbulent dense jets. Environ Process 6:525–541. https://doi.org/10.1007/s40710-019-00359-w
24. Roberts PJW, Toms G (1987) Inclined dense jets in flowing current. J Hydraul Eng 113(3):323–341. https://doi.org/10.1061/(ASCE)0733-9429(1987)113:3(323)
25. Roberts PJW, Ferrier A, Daviero G (1997) Mixing in inclined dense jets. J Hydraul Eng 123(8):693–699. https://doi.org/10.1061/(ASCE)0733-9429(1997)123:8(693)
26. Seo I, Kim H, Yu D, Kim D (2001) Performance of tee diffusers in shallow water with crossflow. J Hydraul Eng ASCE. https://doi.org/10.1061/(ASCE)0733-9429(2001)127:1(53)
27. Shao DD, Law AWK, Li HY (2008) Brine discharges into shallow coastal waters with mean and oscillatory tidal currents. J Hydro-Environ Res 2(2):91–97. https://doi.org/10.1016/j.jher.2008.08.001
28. Shao DD, Law AWK (2010) Mixing and boundary interactions of 30° and 45° inclined dense jets. Environ Fluid Mech 10(5):521–553. https://doi.org/10.1007/s10652-010-9171-2
29. Zeitoun MA, McIlhenny WF (1971) Conceptual designs of outfall systems for desalination plants. In: Offshore technology conference, Houston, p 12. https://doi.org/10.4043/1370-MS
30. Zhang W, Zhu DZ (2011) Near-field mixing downstream of a multiport diffuser in a shallow river. J Environ Eng 137(4):230–240. https://doi.org/10.1061/(ASCE)EE.1943-7870.0000327
31. Zhang S, Law AWK, Jiang M (2017) Large eddy simulations of 45° and 60° inclined dense jets with bottom impact. J Hydro-Environ Res 15:54–66. https://doi.org/10.1016/j.jher.2017.02.001

Publisher's Note Springer Nature remains neutral with regard to jurisdictional claims in published maps and institutional affiliations.